Predicting RF Path Loss in Forests Using Satellite Measurements of Vegetation Indices

Sujuan Jiang
Dept. of
Computing Science
University of Alberta
sujuan@ualberta.ca

Carlos Portillo-Quintero
Dept. of Earth and
Atmospheric Science
University of Alberta
portillo@ualberta.ca

Arturo Sanchez-Azofeifa
Dept. of Earth and
Atmospheric Science
University of Alberta
gasanche@ualberta.ca

Mike H. MacGregor
Dept. of
Computing Science
University of Alberta
mike.macgregor@ualberta.ca

Abstract—We report preliminary results from a novel method that predicts the value of the RF path loss exponent (PLE) from satellite remote-sensing observations. The value of the PLE is required when designing wireless sensor networks for environmental monitoring. The model was produced by correlating field measurements of path loss to Landsat 8 data for three dates in 2013. The correlations are strong ($R^2 > 0.87$), and exhibit high statistical significance ($p < 0.01$). As far as we know, this is the first reported work that links remote sensing observations to field predictions of RF loss.

The work reported here is preliminary because we were only able to gather field observations for three dates in 2013. Now that we know the approach holds some promise, we plan to extend the work with a much more aggressive field campaign in the spring and summer of 2014.

I. INTRODUCTION

Wireless sensor networks (WSNs) have been very actively studied. There is a rich literature of theoretical studies on the abstract properties of WSNs, and algorithms for sensor coverage, sensor placement, relay placement, and base station mobility [1]–[4]. A key issue in designing and deploying WSNs is the RF propagation environment [5], largely because of the limited energy budget at the wireless nodes. RF transmission, and to a lesser extent, signal reception are the main consumers of energy in wireless nodes. Thus, if we can predict the magnitude of RF signal loss in the area to be covered by a WSN, we can develop power budgets for the links between nodes, and estimate the lifetime of the network for given battery resources.

RF propagation through vegetation has been studied at least since the 1960's [6]. One broad class of propagation models is empirical. These are based on experimental measurements of received signal strength, converting these data to attenuation, and regressing against distance. The current ITU-R recommended model for predicting attenuation in vegetation is of this form [7]. The shortcoming of an empirical model is that it has no mechanistic link to the properties of the vegetation in the area of interest. Model parameter values are specific to the site [8] or species investigated [9]. The key parameter in models for RF propagation through vegetation, such as the one recommended by the ITU-R, is the path loss exponent (PLE).

We propose a novel method for predicting PLE values from Landsat 8 remote-sensing observations. At the moment,

our model is specific to aspen boreal forests, which cover approximately 1.5 to 2.0 million square kilometres in Canada alone. The method is generalizable to other forest types, and we propose both broader coverage of boreal forests, and other vegetation types, as future work. The satellite data we use are available for any location on Earth, thus enabling characterization and prediction of the RF propagation environment in forested areas without the need for field measurements. As far as we know, this is the first reported work that links remote sensing observations to field predictions of RF loss.

A second contribution is that we also propose a novel way of predicting high-resolution 30m x 30m Landsat 8 data required by our method from lower-resolution 250m x 250m MODIS observations that are not as easily degraded. Such degradation occurs relatively frequently when cloud cover or aerosols such as pollution or sand storms degrade or significantly interfere with the high-resolution satellite data we are using. We tested our proposal by comparing its predictions to actual values for a date when the 30m x 30m data are available, and the results show absolute errors of less than 5%.

In the following section, we survey the previous work on the general problem of predicting RF loss in vegetation. We note that there is no previously published work linking remote-sensing measurements to link budget analysis. We believe this paper is the first published work on that topic. The survey of related work is followed in Section 3 by a detailed description of our methodology. Section 4 presents our experimental observations and observations for leaf-on and out-of-leaf conditions at a site in Alberta, Canada. Section 5 presents our method for predicting missing high-resolution data from low-resolution satellite observations. Section 6 presents conclusions and future work.

II. PREVIOUS WORK

The topic of RF propagation through vegetation has been of commercial interest since the 1960's due to the importance of wireless links for telephony [6]. The early work was relevant to line-of-sight relay links. The propagation paths of interest are above the forest canopy, between two terminals situated several kilometres apart [10]. While more recently, the topic has become important for the design and location of cellular network towers. Models are required to predict attenuation along the "slant path" between a cellular tower and a user

situated in or travelling through a forested area such as an urban park [8], [11]. Cellular operators also have an interest in predicting the effects of isolated trees or lines of trees, as these are common occurrences in urban landscapes [12].

Propagation paths for WSNs in forested areas are different than for telephony, with both terminals typically being located in or below the canopy. Paths are usually roughly horizontal, following the terrain. There are some applications that need to characterize vertical paths, such as measurements being conducted in tree crowns [5]. In any case, the unpredictability of RF signal strength is a major issue in the design of WSNs [5]. Attenuation predictions are needed both statically as a function of distance, and dynamically as a function of wind, weather, and vegetation condition (leaf-on or out-of-leaf).

Several mechanistic models of RF attenuation in vegetation have been developed [12], [13]. Below about 200 MHz, where the dimensions of the vegetation are much smaller compared to the wavelength of the RF signal, a dissipative slab model can be used [6]. Above this frequency, from 200 MHz to 2 GHz, Cavalcante et al. proposed a four-layer slab model. This consists of a semi-infinite ground plane supporting above it a trunk layer, canopy layer, and air layer [14]. Models like these require numerical methods for solution, and depend on the values for several parameters in each layer (permittivity, conductivity and permeability). Their chief advantage over empirical models is that they provide physical insight into wave characteristics and propagation modes [13].

The ITU-R in Recommendation P.833 [7] recommends an empirical model, rather than a mechanistic one. Common empirical models predict an exponential decrease in signal strength with both distance and frequency [9], [12]. The ITU-R Recommendation is a good starting point for the general form of empirical predictions, but in itself is not sufficient for WSN design, directed as it is towards paths that traverse the forest canopy, rather than tree trunks and understory vegetation [15]. The parameters in the Recommendation are also of limited applicability, as they are tied to specific species of trees that may or may not be present in a given area of interest. In addition, the parameter values are for a single species at a particular density. There is no guidance in the Recommendation for sites consisting of a mixture of species of varying densities or degrees of canopy openness.

Our goal is to extend models of the form recommended by the ITU-R to heterogeneous forests consisting of a mixture of species at varying densities. Our contributions are:

- exploration and demonstration of a significant correlation between the value of the path loss exponent, and the values of remotely sensed vegetation indices (VIs). The global availability of high-resolution 30m x 30m satellite data for these indices thus enables RF path loss predictions for WSNs anywhere in the world.

- demonstration of a method for predicting high-resolution VI values from low-resolution 250m x 250m MODIS data. This enables us to fill in gaps in the temporal series of VI values when the satellite view of the area of interest is obscured by clouds or aerosols.

III. METHODOLOGY

The basic model for the attenuation of RF signals with distance, also called free space path loss, is:

$$P_r(d) = P_t \times G_r G_t (\frac{\lambda}{4\pi d})^2 \qquad (1)$$

where P_r and P_t are the received and transmitted power in mW, d is the distance from the transmitter to the receiver in meters, G_r and G_t are the gain of the receive and transmit antennas, and λ is the wavelength in meters. Defining $K = G_r G_t (\lambda/4\pi)^2$ leads to:

$$P_r(d) = K \times P_t/d^2 \qquad (2)$$

K is determined by the gain of the receive and transmit antennas, their connection to the respective radio, and the frequency of operation. The value of K is fixed once the radios and antennas have been selected and interconnected and does not change with variation of vegetation.

We apply this variation of the free space path loss equation alone, and do not consider the potential effects of multi-path propagation within the forest. Previous work sponsored by the UK Radiocommunications Agency [9] found that multi-path propagation is not a significant factor in forests as long as the trees are in-leaf. That is the condition we consider in this work.

For areas with varying vegetation densities, we replace the fixed value of 2 in the exponent of d with the path loss exponent α, where densely forested areas have high values of α, and sparsely forested areas have low values:

$$P_r(d) = K \times P_t/d^\alpha \qquad (3)$$

Our objective is to characterize the relationship between path loss exponent, α, and vegetation density. α can be obtained from signal loss measurements in the field, in the area of interest. Vegetation density is usually represented by vegetation indices (VIs) such as Normalized Difference Vegetation Index (NDVI). NDVI assesses whether the observed area contains live green vegetation or not and has a value ranging from -1 to 1. Negative values correspond to water. Very low values (0.1 and below) represent barren areas like rock, sand, or snow. Moderate values (0.2 and 0.3) correspond to shrub and grassland. High values indicate densely vegetated areas including temperate and tropical rainforests (0.6 to 0.8). Other vegetation indices including Simple Ratio (SR), and Atmospherically Resistant Vegetation Index (ARVI) also reflect the vegetation density. The equations defining these indices are given in Eq. 4 through Eq. 7. The variables ρ_{nir}, ρ_r and ρ_b represent reflectance of the near infrared, red, and blue band. γ is used to minimize the atmospheric effects and usually set to 1.0.

$$SR = \rho_{nir}/\rho_r \qquad (4)$$
$$NDVI = (\rho_{nir} - \rho_r)/(\rho_{nir} + \rho_r) \qquad (5)$$
$$ARVI = (\rho_{nir} - \rho_{rb})/(\rho_{nir} + \rho_{rb}) \qquad (6)$$
$$\rho_{rb} = \rho_r - \gamma * (\rho_b - \rho_r) \qquad (7)$$

We calculate the vegetation index values from Landsat 8 Operational Land Imager (OLI) satellite data for each 30m x 30m cell in an area of interest. Table I gives the bands and wavelengths sensed by Landsat 8 OLI.

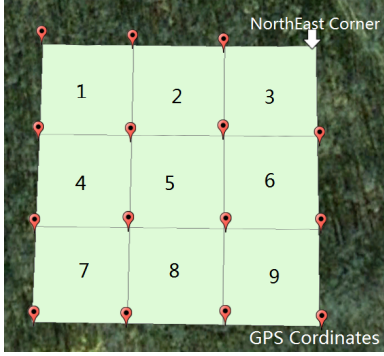| Bands	Wavelength (micrometers)
Band 1 - Coastal aerosol	0.43 - 0.45
Band 2 - Blue	0.45 - 0.51
Band 3 - Green	0.53 - 0.59
Band 4 - Red	0.64 - 0.67
Band 5 - Near Infrared (NIR)	0.85 - 0.88
Band 6 - SWIR 1	1.57 - 1.65
Band 7 - SWIR 2	2.11 - 2.29
Band 8 - Panchromatic	0.50 - 0.68
Band 9 - Cirrus	1.36 - 1.38

TABLE I.   LANDSAT 8 OLI BANDS [16]

Fig. 1.   Grid of Study Area

IV.   FIELD MEASUREMENTS

We made field trips to the Ministik Game Bird Sanctuary on July 23, August 21, and October 11, 2013. The Sanctuary locates in the east of Edmonton, Alberta, Canada. Vegetation includes Boreal mixed-wood forest, Populus balsamifera, and Trembling Aspen. The forest has a dense understory with almost no conifers.

We took signal loss measurements in a rectangular 90m x 90m area of interest. The grid was oriented along the cardinal directions, with its northeast corner at UTM co-ordinates 12U 366975E 5907915N. We note that UTM co-ordinates are in units of meters. The grid is shown on the map in Figure 1. We divided the grid into nine 30m x 30m cells to match the pixel size of the available Landsat 8 satellite data.

Determining K

Our first experiment was to make two sets of measurements at several distances along straight lines in two different areas. The vegetation density, and thus α, was roughly constant in each of the two areas, with the second area being denser than the first. Portable GPS receivers (Garmin model 62S) with WAAS enabled were used to set the measurement positions. Libelium Waspmotes with Digi International Xbee Pro S1 radios at 2.4GHz operating frequency and 2.1 dBi whip antennas were used for the transmitter and receiver. Special-purpose software was written for the transmitter to transmit packets, and for the receiver to detect the RSSI value in dBm and display it on an attached laptop. Ten values for RSSI were collected at each distance, and averaged for the final result in each cell. The radio and antenna configurations were kept the same for these two sets of measurements, so while we expected α to differ, K was physically constrained to remain the same. These

measurements were the raw data from which we calculated K (see Table II, Figure 2 and Figure 3).

By taking logarithms on both sides of Eq. 3, we get

$$\log P_r(d) = -\alpha * \log d + \log K + \log P_t \qquad (8)$$

where the transmitted power P_t of the Waspmotes is a constant, 63mW, and by taking ten times the logarithm of received power $P_r(d)$, it equals the measured RSSI. We used a least squares regression to find the values of K and α that best explained the two sets of measurements. We allowed α to be different in the two areas, but forced K to be the same. We found the value of $\log K$ to be -5.9. In the denser area, α had a value of 3.2, while in the sparser area it was 2.4.

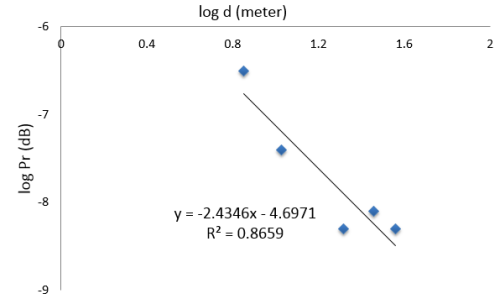| Line 1 - sparse		Line 2 - dense	
distance (m)	RSSI	distance (m)	RSSI
7.07	-65	1.414	-65
10.63	-74	4.47	-76
20.00	-91	5.00	-77
20.81	-83	11.31	-74
28.64	-81	16.12	-87
36.07	-83	20.00	-83

TABLE II.   RSSI MEASUREMENTS USED TO FIND K
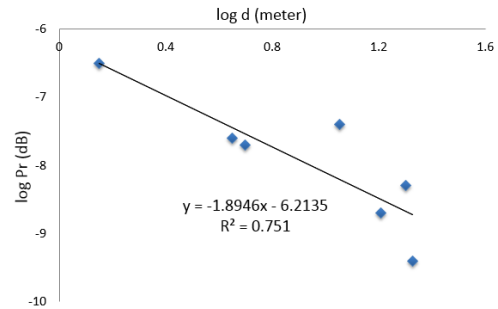

Fig. 2.   RSSI in the Sparse Area

Fig. 3.   RSSI in the Dense Area

Measuring RSSI

Our second set of experiments was to record the received signal strength indication, RSSI in dBm, on a diagonal path across each cell. We made three separate field trips, in July, August, and October, to gather data under different vegetation conditions. We used the same equipment configuration as for the determination of K. We used the previously determined value for K plus the RSSI data to calculate the value of α for each cell, under the vegetation conditions on the date of the

Cell	July			August			October		
	RSSI	α	NDVI	RSSI	α	NDVI	RSSI	α	NDVI
1	-94	3.256	0.798	-98	3.502	0.759	-90	3.010	0.431
2	-101	3.686	0.806	-98	3.502	0.753	-89	2.949	0.386
3	-100	3.625	0.819	-94	3.256	0.749	-88	2.888	0.386
4	-97	3.440	0.811	-95	3.318	0.763	-88	2.888	0.453
5	-98	3.502	0.826	-89	2.945	0.738	-96	3.380	0.352
6	-101	3.686	0.846	-96	3.379	0.747	-93	3.195	0.361
7	-94	3.256	0.803	-95	3.318	0.750	-92	3.133	0.423
8	-95	3.318	0.837	-90	3.035	0.742	-96	3.379	0.373
9	n/a	n/a	0.838	-98	3.502	0.751	-93	3.195	0.357

TABLE IV.   CELL DATA

measurements. One pair of diagonally opposite corners of each cell were used to make each measurement. Each cell covers one pixel in the Landsat 8 images of the area, so these corner-to-corner measurements cover the smallest useful distance. In effect, the resolution of the satellite image sets the spatial resolution for our path loss predictions.

Predicting missing VI measurements

One of the potential drawbacks of relying on satellite data in the visible spectrum is that clouds and aerosols can interfere with the satellite's view of the ground. To alert users to this problem, Landsat 8 data products include an indication of the cloudiness of the view of the area of interest on the day each image is obtained. For August and October, these values were 2.36 and 3.45, respectively. However, for July, the cloudiness index was 13.15. This is extremely high, making the VI calculations for that date unreliable. To solve the problem of missing satellite data, we tested the use of lower resolution MODIS satellite data having 250m x 250m pixels to predict the July Landsat 8 data from the May and September Landsat 8 data, following the same trend as the change in the encompassing MODIS pixel. That is, if L denotes Landsat 8 values, M denotes MODIS values, and if the subscripts 1, 2 and 3 denote three successive dates, then:

$$L_2 = L_1 + (L_3 - L_1) * (M_2 - M_1)/(M_3 - M_1) \quad (9)$$

where date 2 is the date when the missing Landsat 8 values are encountered. We first tested this method by comparing the values it predicts for a date when the Landsat 8 data are available. We used MODIS and Landsat 8 data from May 20, August 24 and September 9. The actual and predicted Landsat 8 values are shown in Table III. The maximum error is 4.9%. We then applied this method to calculate the missing NDVI values for our July 23 field trip (Table IV).

cell	Actual	Predicted
1	0.7439	0.7587
2	0.7454	0.7643
3	0.7538	0.7759
4	0.7571	0.7719
5	0.7517	0.7776
6	0.7498	0.7864
7	0.7623	0.7695
8	0.7693	0.7874
9	0.7631	0.7893

TABLE III.   ACTUAL AND PREDICTED NDVI VALUES FOR AUGUST 24

The raw RSSI data for all three field trips is shown in Table IV, along with the values for α calculated from Eq. 8, and the Landsat 8 NDVI of each cell. During our first field trip in July, laptop power constraints prevented us from collecting RSSI data for the ninth cell. The NDVI values shown for July are the predicted values from Eq. 9.

V.   RESULTS AND DISCUSSION

We tested linear, logarithmic, and quadratic equations for their fit to the data (see Fig. 4 - 6). We use two figures of merit, R^2 and p, to assess how well each correlation fits a particular data set. The coefficient of determination, R^2, indicates how well a set of data points fit a regression equation. The closer the value of R^2 is to one, the better the regression equation fits

the data. The statistical significance of the correlation is $(1-p)$ so that smaller values for p are better. The R^2 and p values for all the NDVI models we tested are shown in Table V.
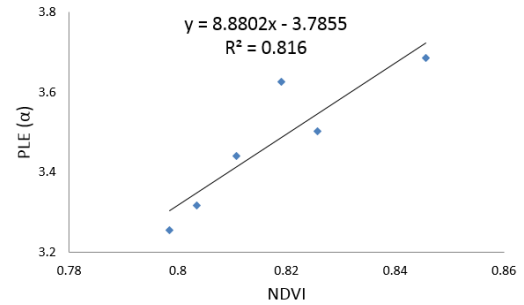

Fig. 4.   Linear fit of α vs. NDVI in July
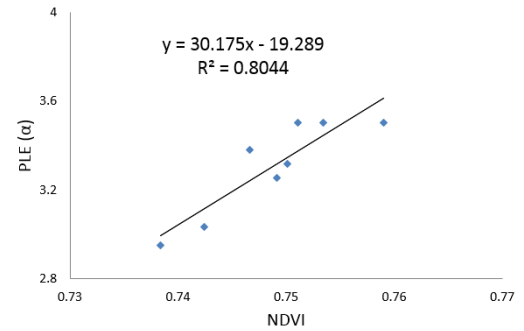

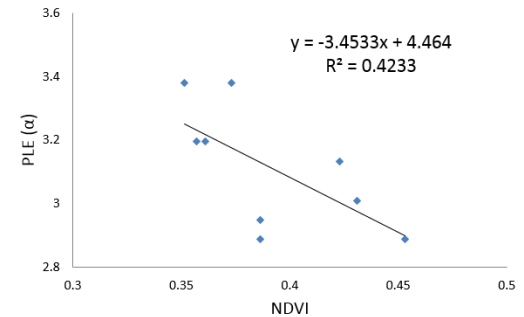Fig. 5.   Linear fit of α vs. NDVI in August

Fig. 6.   Linear fit of α vs. NDVI in October

For the July and August data, we found that the simplest model, the linear function, fits NDVI and other vegetation indices such as ARVI and SR to α very well. We present the

results for the correlations with NDVI here; those for the other indices behave similarly. It has R^2 values greater than 0.80 and p values of 0.014 or better. The slightly more complex quadratic model fits these data extremely well, and has R^2 values greater than 0.87 and p values of 0.006 or better. The logarithmic model for these data also has very good values of R^2 and p, but they are not significantly better than the simpler linear model.

The correlation for the October data is qualitatively different than for July and August, giving an inverse relationship between α and NDVI. The explanation for this is that by the time we visited the site in October, the trees had dropped their leaves, and the forest was out-of-leaf. This can be observed indirectly from the dramatic change in NDVI values. In July, NDVI ranges from 0.79 to 0.85, and in August, it ranges from 0.74 to 0.76. NDVI values of 0.7 and 0.8 correspond to densely vegetated areas that can largely affect RF propagation. However, in October, NDVI is much lower and ranges from 0.35 to 0.46, which indicates the area is out-of-leaf and RF propagation is no longer affected by vegetation. The satellite sensor, of course, was still receiving reflectance data from the area of interest in October, likely from biomass on the forest floor [17]. We conclude that our proposed method of using NDVI data to predict α is only applicable when the forest is in-leaf. Further work is required to predict path losses in the out-of-leaf condition. As noted earlier, the underlying model would also have to change, as multi-path propagation becomes important in this condition.

To summarize, we found that a quadratic model has the best ability to predict α from satellite NDVI measurements. However, a simpler linear model also performs quite well. This method is applicable only when the forest is in-leaf, although that is satisfactory for link budget calculations, because the in-leaf condition is when the highest path losses are observed.

	Linear		Logarithmic		Quadratic	
	R^2	p	R^2	p	R^2	p
July: α-NDVI	0.8160	0.0136	0.8201	0.0130	0.8812	0.0056
August: α-NDVI	0.8044	0.0025	0.8065	0.0025	0.8677	0.0012
October: α-NDVI	0.4233	0.0577	0.4334	0.0538	0.4766	0.0396

TABLE V.   SUITABILITY OF REGRESSION MODELS

VI.   CONCLUSIONS AND FUTURE WORK

We propose a relatively simple model to predict values for the path loss exponent, α, based on satellite observations of NDVI. We found this approach to work very well for leaf-on conditions in a study site consisting of boreal forest in central Alberta. We also propose a method to fill in missing high-resolution 30m x 30m data for dates where the satellite's view of the area of interest is obscured by clouds or aerosols. Based on these promising initial results, we plan to carry out a much lengthier field campaign from April through October of 2014. This will enable us to develop a method for predicting PLE values from NDVI measurements for the entire leaf-on phase in boreal forest sites.

Lastly, the authors would like to note that even for this relatively small field study, substantial planning, as well as patience with weather and equipment was required. The step from computer simulations and laboratory tests to real fieldwork in a dense, buggy and sometimes wet forest is a substantial one. We believe it has also been very rewarding.

REFERENCES

[1] K. Y. Kaneshiro, M. H. Kido, C. W. Mundt, K. N. Montgomery, A. Asquith, and D. W. Goodale, "Integration of wireless sensor networks into cyberinfrastructure for monitoring Hawaiian "mountain-to-sea" environments." *Environmental Management*, vol. 42, no. 4, pp. 658–666, 2008.

[2] X. Han, X. Cao, E. Lloyd, and C.-C. Shen, "Fault-tolerant relay node placement in heterogeneous wireless sensor networks," *IEEE Transactions on Mobile Computing*, vol. 9, no. 5, pp. 643–656, May 2010.

[3] E. Oyman and C. Ersoy, "Multiple sink network design problem in large scale wireless sensor networks," *2004 IEEE Int'l Conf. on Communications*, pp. 3663–3667 Vol.6, 2004.

[4] Y. Türkogullari, N. Aras, I. Altinel, and C. Ersoy, "An efficient heuristic for placement, scheduling and routing in wireless sensor networks," *Ad Hoc Networks*, vol. 8, pp. 654–667, 2010.

[5] S. Burgess, M. Kranz, N. Turner, R. Cardell-Oliver, and T. Dawson, "Harnessing wireless sensor technologies to advance forest ecology and agricultural research," *Agricultural and Forest Meteorology*, vol. 150, no. 1, pp. 30–37, Jan. 2010.

[6] Y. Meng, Y. Lee, and B. Ng, "Study of propagation loss prediction in forest environment," *Progress In Electromagnetics Research B*, vol. 17, pp. 117–133, 2009.

[7] ITU-R, "ITU-R Recommendation P.833-7 Attenuation in Vegetation," 2012.

[8] M. H. C. Dias and M. S. de Assis, "An empirical model for propagation loss through tropical woodland in urban areas at UHF," *IEEE Trans. on Antennas and Propagation*, vol. 59, no. 1, pp. 333–335, Jan. 2011.

[9] N. Rogers, A. Seville, J. Richter, and D. Ndzi, "A generic model of 1-60 GHz radio propagation through vegetation-final report," no. May, p. 152, 2002.

[10] I. Kovács, P. Eggers, and K. Olesen, "Radio channel characterisation for forest environments in the VHF and UHF frequency bands," in *Vehicular Technology Conference*, no. 3, 1999, pp. 1387–1391.

[11] J. Voldhaug, "Deployable WiMAX in a forest area; channel measurements and modelling," in *2010 Military Communications Conference*, 2010, pp. 737–742.

[12] Y. Meng and Y. Lee, "Investigations of foliage effect on modern wireless communication systems: A review," *Progress In Electromagnetics Research*, vol. 105, pp. 313–332, 2010.

[13] L.-W. Li, T.-S. Yeo, P.-S. Kooi, and M.-S. Leong, "Paths through a four-layered model of rain forest : An analytic approach," *IEEE Trans. on Antennas and Propagation*, vol. 46, no. 7, pp. 1098–1111, 1998.

[14] G. Cavalcante and A. Giarola, "Optimization of radio communication in media with three layers," *IEEE Trans. on Antennas and Propagation*, vol. 31, no. 1, pp. 141–145, 1983.

[15] I. Cuinas, J. Gay-Fernandez, P. Gomez, A. V. Alejos, and M. G. Sanchez, "Radioelectric propagation in mature wet forests at 5.8 GHz," in *2009 IEEE Antennas and Propagation Society International Symposium*. IEEE, Jun. 2009, pp. 1–4.

[16] B. Markham, E. Knight, B. Canova, E. Donley, G. Kvaran, K. Lee, J. Barsi, J. Pedelty, P. Dabney, and J. Irons, "The Landsat data continuity mission operational land imager (OLI) sensor," in *2012 IEEE Int'l Geoscience and Remote Sensing Symposium (IGARSS)*, 2012, pp. 6995–6998.

[17] K. Huemmrich, T. Black, P. Jarvis, J. McCaughey, and F. Hall, "High temporal resolution NDVI phenology from micrometeorological radiation sensors," *Journal of Geophysical Research*, vol. 104, no. D22, pp. 27 935–27 944, Nov. 1999.